

DIFFERENTIAL CROSS SECTION RESULTS FROM NUTEV

VOICA A. RADESCU

for the NuTeV Collaboration

University of Pittsburgh,

Pittsburgh, PA 15260, USA

E-mail: voica@farfalle.phyast.pitt.edu

The NuTeV experiment has collected high statistics, high energy samples of ν and $\bar{\nu}$ charged-current interactions using the sign-selected Fermilab neutrino beam. NuTeV has extracted ν and $\bar{\nu}$ differential cross sections for DIS single-muon production at moderate $x > 0.015$ and average $Q^2 \sim 15 \text{ GeV}^2$. Differential cross sections and structure function results are presented. The NuTeV measurement has improved systematic precision and includes data over an expanded kinematic range up to high inelasticity.

1 Introduction

Neutrino deep inelastic scattering (DIS) is a versatile probe of nucleon structure. The general form of the differential cross sections for the neutrino–nucleon charged-current process depends upon three Lorentz-invariant structure functions that parametrize the structure of the nucleon: $2xF_1$, F_2 , xF_3 :

$$\frac{d^2\sigma^{\nu(\bar{\nu})}}{dx dy} = \frac{G_F^2 M E_\nu}{\pi} \left[(1-y)F_2^{\nu(\bar{\nu})} + \frac{y^2}{2}2xF_1^{\nu(\bar{\nu})} \pm y \left(1 - \frac{y}{2}\right) xF_3^{\nu(\bar{\nu})} \right] \quad (1)$$

where G_F is Fermi weak coupling constant, M is the nucleon mass, E_ν is the incident neutrino energy, and y the inelasticity. Structure function xF_3 is unique to neutrino interactions because neutrinos interact only weakly. Structure functions depend on x , the Bjorken scaling variable and Q^2 , the square of the four-momentum transfer to the nucleon. In neutrino scattering the Lorentz-invariant kinematic variables x , y and Q^2 are constructed from three measured quantities: the momentum of the outgoing muon, p_μ , the angle of the outgoing muon with respect to the beam direction, θ_μ , and the energy of the outgoing hadrons, E_{had} .

NuTeV is a fixed target deep inelastic neutrino-scattering experiment which collected data during 1996-97 (Fermilab) using an iron-scintillator neutrino detector [1]. There are two important and improved features which make NuTeV the most precise experiment to date. First unique feature is the use of Sign Selected Quadrupole Train (SSQT) beam to produce a high purity neutrino or, alternatively, anti-neutrino beam. The other special feature is the use of a continuous calibration beam running concurrently with data-taking, which enables the NuTeV experiment to considerably improve its knowledge of the energy scale and detector response functions. Muon energy scale was measured to 0.7% and hadron energy scale to 0.43%.

2 Cross Section Measurements and Comparisons

The differential cross section per nucleon on iron as function of x , y and E_ν can be expressed in terms of the relative flux as function of energy and differential number of charged current events:

$$\frac{d^2\sigma^{\nu(\bar{\nu})}(E_\nu)}{dx dy} = \frac{1}{\Phi(E_\nu)} \frac{d^2N^{\nu(\bar{\nu})}(E_\nu)}{dx dy}. \quad (2)$$

The data selection criteria for the main cross section sample requires a good muon track for accurate momentum measurement, event containment and minimum energies thresholds: $E_{had} > 10$ GeV, $E_\mu > 15$ GeV and $E_\nu > 30$ GeV. To minimize the effects of the non-perturbative contributions kinematic cuts of $Q^2 > 1\text{GeV}^2$ and $x < 0.70$ are required.

The SSQT allows NuTeV to expand the data sample of toroid-analyzed events to include previously inaccessible data of low energy muons which stop inside the detector. Those events are reconstructed using exclusively information from their energy deposition in the target calorimeter. This is a new sample and it is treated separately. For this sample we require good containment and $E_\mu > 4$ GeV.

Neutrino relative flux is determined from a nearly independent sample at low hadronic energy ($E_{had} < 20$ GeV) using the ‘‘fixed ν_0 method’’: as $y = \frac{E_{had}}{E_\nu} \rightarrow 0$ the integrated number of events is proportional to the flux. The absolute flux is obtained by normalizing the cross section to the world average $\nu - Fe$ cross section value of $\sigma^\nu/E_\nu = 0.677 \pm 0.014 \times 10^{-38} \text{cm}^2/\text{GeV}$ [2]. A detector simulation is used to account for acceptance and resolution effects and employs as input a (LO)QCD inspired cross section model which is iteratively fit to the data until convergence occurs (within 3 loops).

Figure 1 shows the extracted differential cross sections for $\nu - Fe$ and $\bar{\nu} - Fe$ as function of y for a representative sample of x bins at $E_\nu = 45$ GeV and $E_\nu = 150$ GeV. The NuTeV data over an extended y region is compared to other neutrino measurements: CCFR [3] and CDHSW [4]. The solid curve is the parametrization fit to the NuTeV data used for calculation of acceptance and smearing corrections [5]. The main systematics due to energies scales and flux determination have been included for NuTeV major data sample, while they still need to be evaluated for the new high- y sample.

For low and moderate x there is good agreement among the data sets over whole energy and y range in both neutrino modes. At high x NuTeV is systematically above the CCFR measurement over the entire energy range. This difference increases with x reaching up to 20% at $x = 0.65$. NuTeV result is similar in level, but different in shape with CDHSW, a data set with large uncertainties. The main difference between NuTeV and CCFR experiments, which are very similar in design and analysis method, is that NuTeV beam was sign selected; it had separate running of neutrinos and, respectively, anti-neutrinos. Having this advantage, NuTeV was always set to focus the muon from the primary vertex, whereas CCFR had simultaneous neutrino and anti-neutrino runs, so that the toroid polarity was reversed periodically to focus either μ^+ or μ^- .

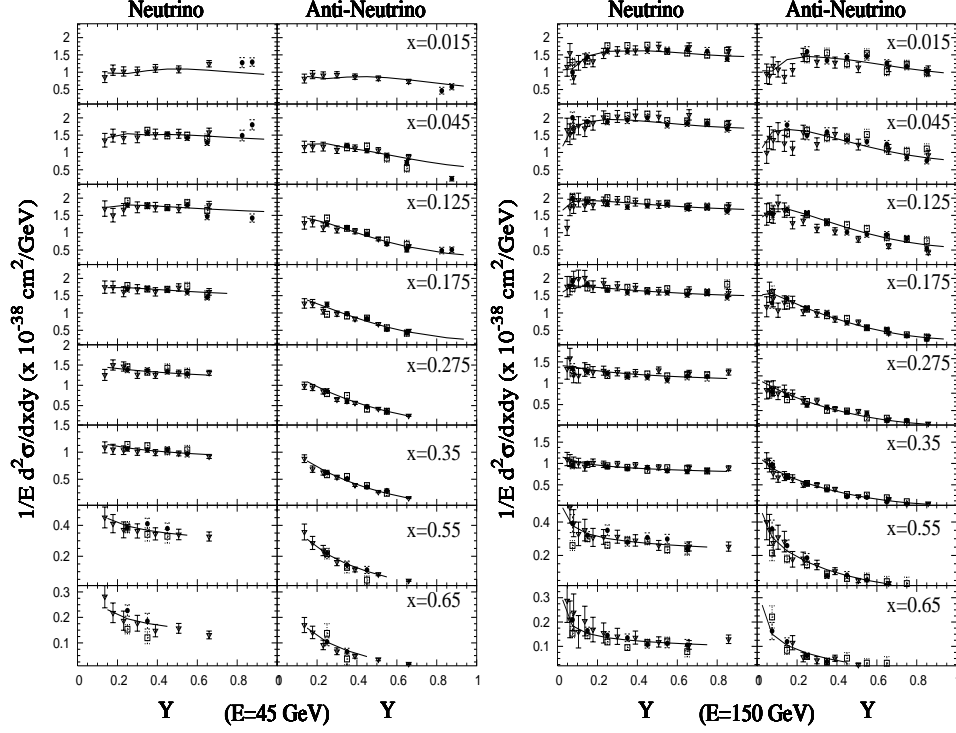


Figure 1. Plots display $\nu - Fe$ and $\bar{\nu} - Fe$ differential cross sections as function of y at $E_\nu = 45 GeV$ (left) and $E_\nu = 150 GeV$ (right) over various x bins. NuTeV data over the extended y region is shown with filled circles, CCFR set is marked with open squares and CDHSW data is displayed with open triangles. The solid curve is the parametrization fit to NuTeV data. The main systematics are included for all NuTeV data points apart from the new high- y sample.

3 Structure Function Measurements and Comparisons

Structure functions can be extracted from fits to linear combination of ν and $\bar{\nu}$ differential cross sections, which have been corrected for 5.67% excess of neutrons over protons in the NuTeV iron target and for QED radiative effects [9]. In this analysis we have not included the cross section points from the high- y sample. The sum of the neutrino and anti-neutrino differential cross sections for charged current interactions on an iso-scalar target is related to the structure function $F_2(x, Q^2)$ by:

$$\frac{d^2\sigma^\nu}{dx dy} + \frac{d^2\sigma^{\bar{\nu}}}{dx dy} = \frac{2MG_F^2 E_\nu}{\pi} \left[\left(1 - y - \frac{Mxy}{2E} + \frac{1 + \left(\frac{2Mx}{Q}\right)^2 y^2}{1 + R_L} \right) F_2 + y \left(1 - \frac{y}{2} \right) \Delta x F_3 \right] \quad (3)$$

where $R_L(x, Q^2) = \frac{\sigma_L}{\sigma_T}$ is the ratio of the cross section for scattering from longitudinally to transversely polarized -bosons, and $\Delta x F_3 = xF_3^\nu - xF_3^{\bar{\nu}} \sim 4x(s - c)$ is sensitive to heavy flavors. The structure function F_2 is determined by performing a one-parameter fit which requires input models for $R_L(x, Q^2)$ and $\Delta x F_3(x, Q^2)$. For $R_L(x, Q^2)$ we use a fit to the world's data [11], and for $\Delta x F_3(x, Q^2)$ we use a NLO QCD model of Thorne-Roberts VFS [10].

Similarly, the difference between neutrino and anti-neutrino differential cross sections is related to the structure function $xF_3(x, Q^2)$ as follows:

$$\frac{d^2\sigma^\nu}{dx dy} - \frac{d^2\sigma^{\bar{\nu}}}{dx dy} = \frac{2MG_F^2 E_\nu}{\pi} \left(y - \frac{y^2}{2} \right) xF_3(x, Q^2) \quad (4)$$

Because $F_2^\nu(x, Q^2) \approx F_2^{\bar{\nu}}(x, Q^2)$, no model inputs are needed to extract xF_3 from one-parameter fit.

Figure 2 shows comparisons of NuTeV measurements of $F_2(x, Q^2)$ and $xF_3(x, Q^2)$ with those from CCFR and CDHSW. The curve on the figure is the fit to NuTeV from our model. The major systematics due to the R_L , ΔxF_3 models, energies scales and flux are included. The differences seen at the cross section level are also reflected in the structure functions. At $x = 0.015$, the lowest x bin, NuTeV is systematically above CCFR by $\approx 3\%$. At the intermediate x , $0.015 < x < 0.5$, all data sets are in good agreement. In the high x region, $x > 0.5$, NuTeV is consistently above CCFR data up to $\approx 20\%$ at $x = 0.65$, and agrees in level, but not in shape with less precise CDHSW data set.

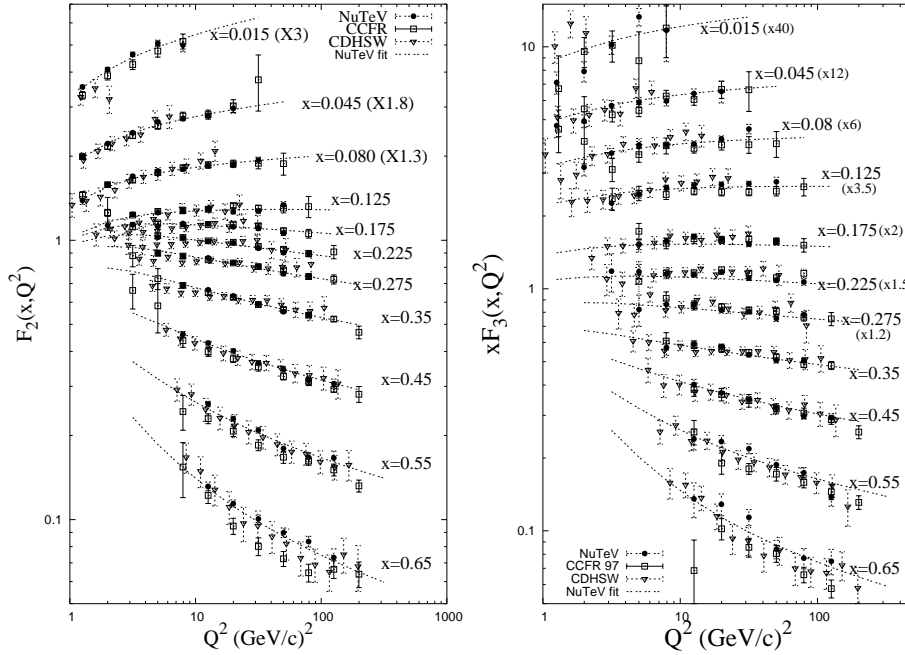


Figure 2. Plots show NuTeV measurements of $F_2(x, Q^2)$ (left) and $xF_3(x, Q^2)$ (right), filled circles, compared to CCFR, open squares, and CDHSW, triangles as function of Q^2 over all x bins. Systematic errors are included. The curve is NuTeV model

Figure 3 shows the ratios of the NuTeV and CCFR F_2 measurements to various NLO QCD models which include an improved treatment of massive charm production: TR-VFS models [10] with MRST-99, MRST-2001 E parton distribution functions sets and ACOT-FFS model with CTEQ4HQ [8]. NuTeV data is significantly above the theory curves at high- x reaching $\approx 15\%$ difference at $x = 0.65$, while the CCFR result is slightly below the curves.

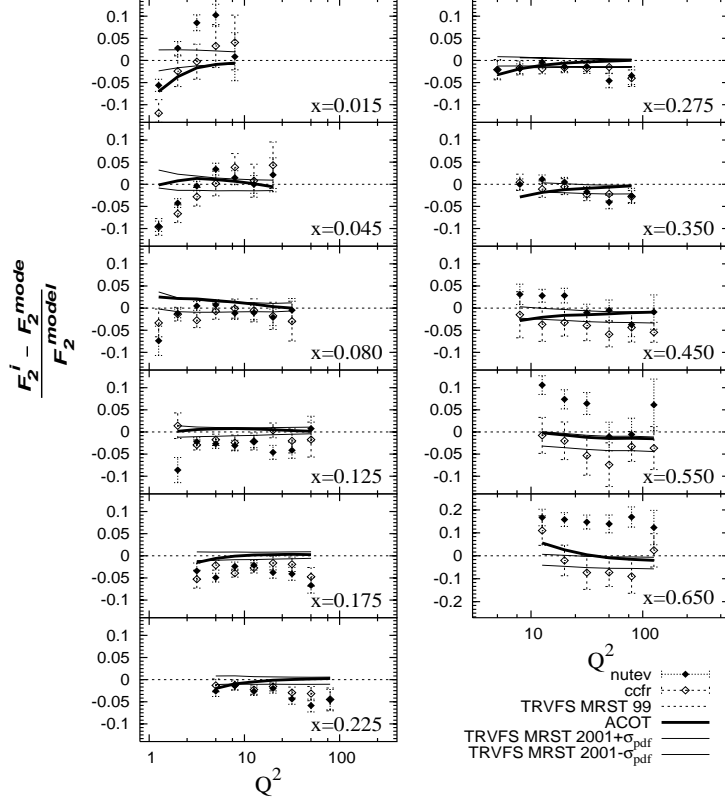


Figure 3. Plots show ratios of the NuTeV (filled diamonds) and CCFR (open diamonds) $F_2(x, Q^2)$ measurements to TR-VFS(MRST-99 pdf) model (dashed line) as function of Q^2 over x bins. The ratio of the ACOT (CTEQ4HQ pdf) (bold curve) and TR-VFS (MRST 2001 E pdf) with $\pm 1\sigma$ uncertainties in pdf's (thin curves) to the TR-VFS(MRST-99 pdf) model are also shown.

In order to compare neutrino measurements to the theory models, one must to correct the theory for target-mass effects [12] and for nuclear effects which are important at low and high x . The nuclear corrections are measured in charged lepton experiments from nuclear targets and the standard way is to use the same correction for neutrino scattering. We use a parametrization independent of Q^2 fit to data [2] which is dominated at $x > 0.4$ by SLAC, a data set with lower Q^2 than NuTeV. The size of the correction ranges from $\approx 10\%$ at $x = 0.015$, is small at intermediate x , and increases from $\approx 7\%$ at $x = 0.45$ to $\approx 15\%$ at $x = 0.65$.

Currently there is a new analysis underway with JLAB data using the Nachtmann variable $\xi = 2x/(1 + \sqrt{1 + 4M^2x^2/Q^2})$, which favors slightly smaller nuclear corrections [13]. We also compare our measurements in the high- x region to SLAC and BCDMS deuterium data sets [6],[7]. In order to compare $F_2^{\nu N}$ from $\nu - Fe$ DIS to the F_2^{lD} from $e(\mu) - D_2$ scattering it is necessary to apply two corrections: for the quark charges seen by the electromagnetic interaction versus the weak interaction and for the difference in light versus heavy target effects. Figure 4 shows the ratios of the NuTeV model to each data set at high x region. NuTeV measurements differ from BCDMS by $\approx 5\%$ and from SLAC by $\approx 10\%$ at $x = 0.65$, which could indicate that neutrino scattering favors smaller nuclear effects at high x .

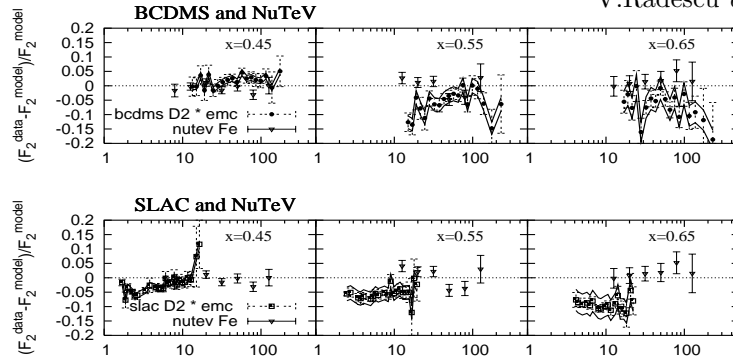


Figure 4. Ratio plots of NuTeV (triangles) and BCDMS D_2 (squares) F_2 measurements to NuTeV model are displayed as function of Q^2 for high- x bins. The ratio plots of NuTeV (triangles) and SLAC D_2 (circles) F_2 measurements to NuTeV model are also shown. The error band on the charged lepton data is the uncertainty of the nuclear correction.

4 Conclusions

We have presented the most precise measurements of neutrino and anti-neutrino differential cross sections to date^a. The sign-selected beam allows NuTeV to include a previously inaccessible high- y data sample in the cross section. The measurements are in good agreement with previous neutrino results over the intermediate x range, but NuTeV results are systematically higher at high- x over the entire energy and y range. The NuTeV measurements of F_2 are also compared to various NLO QCD models and in the high x region the results are systematically above theory curves, from 5 to 15%. Assumptions for the nuclear corrections have been made when compared to the theory models and charged lepton data. The preliminary result is available on NuTeV web-page [14].

References

1. D. A. Harris *et al.*, Nucl. Instrum. Methods **A 447** (2000) 377 (hep-ex/9908056).
2. W. Seligman, Ph. D. Thesis, Columbia University, Nevis 292 (1997).
3. U. K. Yang, Ph. D. Thesis, University of Rochester, (2001).
4. P. Berge *et al.*, Z. Phys. **C** (1991) 187.
5. A. J. Buras and K. L. F. Gaemers, Nucl. Phys. **B 132** (1978) 2109.
6. L. W. Whitlow *et al.*, Phys. Lett. **B 282** (1995), 433.
7. A. C. Benvenuti *et al.*, Phys. Lett. **B 237** (1990), 592.
8. M. A. G. Aivazis, J. C. Collins, F. I. Olness and W. K. Tung Phys. Rev. **D 50**, (1994) 3102 (hep-ph/9312319).
9. Bardin, D. Y. and Dokuchaeva, JINR-E2-86-260 (1986).
10. R. S. Thorne and R. G. Roberts, Phys. Lett. **B 421** (1998) 303 (hep-ph/9711223); A. D. Martin *et al.* Eur. Phys. J. **C 18** (2000) 117 (hep-ph/0007099).
11. L. W. Whitlow *et al.*, Phys. Lett. **B 250** (1990) 193.
12. H. Georgi and H. D. Politzer, Phys. Rev **D 14** (1976) 1829.
13. J. Arrington *et al.*, nucl-ex/0307012v2 (2003).
14. NuTeV website: www-nutev.phyast.pitt.edu/results_2004/nutev_sf.html

^aThe figures in this proceedings have been recently updated and they contain minor changes to the results presented at the conference.